ORGANIC PROCESS RESEARCH & DEVELOPMENT
OPR&D
Article
Cite This: Org. Process Res. Dev. XXXX, XXX, XXX−XXX
pubs.acs.org/OPRD

A Tailor-Made Self-Sufficient Whole-Cell Biocatalyst Enables Scalable Enantioselective Synthesis of (*R*)-3-Quinuclidinol in a High Space-Time Yield

Qian Chen,[†] Baogang Xie,[‡] Liping Zhou,[†] Lili Sun,[†] Shanshan Li,[†] Yuhan Chen,[†] Shan Shi,[†] Yang Li,[†] Mingan Yu,[†] and Wei Li*[,†]

[†]Department of Medicinal Chemistry, School of Pharmacy, Chongqing Medical University, Chongqing 400016, PR China
[‡]Office of School of Pharmacy, Chongqing Medical University, Chongqing 400016, PR China

Supporting Information

ABSTRACT: A self-sufficient two-in-one whole-cell biocatalyst combining ketoreductase and cofactor regenerating enzyme activities has been developed and successfully utilized to synthesize (*R*)-3-quinuclidinol with an increase in the reaction rate of 3-fold over the native enzymes at low biocatalysts loading (∼1.65%), excellent enantioselectivity, impressive substrate concentration of 486 g L^{-1}, and high space-time yield of (*R*)-3-quinuclidinol up to 1505.5 g L^{-1} d^{-1}, which was the highest ever reported. These results demonstrated that the newly developed self-sufficient biocatalyst could be useful for synthetic and industrial application in synthesis of (*R*)-3-quinuclidinol, essential for the production of solifenacin, revatropate, and aclidinium, with better clinical outcome than those currently available.

KEYWORDS: *biocatalyst, (R)-3-quinuclidinol, bifunctional enzymes, self-sufficient, biotransformation*

INTRODUCTION

Enantiopure alcohol can be readily derivatized and further transformed, making it a pivotal building block for synthesis of various compounds, particularly pharmaceutical products.[1−5] (*R*)-3-quinuclidinol is used to produce many commercially available drugs such as solifenacin,[6] aclidinium bromide,[7] revatropate,[8] and palonosetron.[9] It was noteworthy that aclidinium bromide and revatropate were approved for treating chronic obstructive pulmonary disease (COPD) which has been the fourth leading cause of death and kills more than 3 million people worldwide every year.[10] Recently a multicriteria decision analysis of aclidinium and tiotropium demonstrated that aclidinium may be preferred for COPD patients.[11] So an efficient method of enantioselective synthesis of (*R*)-3-quinuclidinol is still essential, and several chemical and biochemical routes have been developed via asymmetric hydrogenation of 3-quinuclidinone using transition-metal chiral catalysts[12,13] or via enzymatic kinetic resolution of racemic mixtures of (DL)-3-quinuclidinol esters.[14] While impressive, these procedures usually suffer from some disadvantages including the high cost of chiral metal catalysts, subsequent removal of trace metals, the oftentimes lengthy process for screening and synthesis ligand, and the unsatisfactory ≤50% yield for enzymatic resolution. To establish a renewable alternative to these chemical processes, biocatalytic routes to (*R*)-3-quinuclidinol using wild-type[15,16] or engineered microorganisms[17−21] have been described. But most of them proceed at low product titer, even only 2 g/L, and needed a prolonged conversion time. A notable exception was the ArQR reductase-catalyzed bioconversion process established by Zhang et al.,[22] which operated at substrate loading of 242 g/L with 100% conversion, 99% ee, and the volumetric productivity of 916 g L^{-1} d^{-1} after 4.5 h, but the thermal stability of ArQR was poor,[23] and using high dosage of lyophilized cells as biocatalysts led to an unfavorable substrate/catalyst ratio.

Considering the high efficiency of the established metal-mediated hydrogenation as the benchmark,[24,25] the biotransformation process not only proceeds at high substrate loadings in the presence of catalytic amount of cofactor or (preferably) without addition of cofactor, but also exhibits high stereoselectivity, productivity, and yield. Gröger et al.[25] described a biocatalytic reduction reaction via enzyme-coupled strategy using "Designer Cells" (coexpressing R or S-specific alcohol dehydrogenase and GDH) without addition of external cofactor (or only in very small amounts in exceptional cases) to furnish a broad range of R and S-alcohols at substrate concentrations of >100 g/L using about 50 g/L cell dosage. Kataoka et al.[26,27] employed *E. coli* BL21(DE3) transformant cells coexpressing carbonyl reductase (S1) and GDH to catalyze the biotransformation of ethyl 4-chloro-3-oxobutanoate (COBE) to ethyl (*S*)-4-chloro-3-hydroxy-butanoate ((*S*)-CHBE) at substrate concentrations of 500 g/L with addition of 0.167 mM $NADP^+$ in a biphasic solvent system, affording 85% molar yield and 100% ee after 34 h reaction. Recently, Xu et al.[28] also described a substrate-coupled method for the production of (*S*)-CHBE, which proceeded at 3 M of COBE in a biphasic system using 140 g/L cell dosage with addition of 0.4 mM $NADP^+$, and 90% yield and 99% ee were obtained after 10 h reaction. Although these biocatalytic processes proceeded at relatively high substrate loading, most of them did not fulfill these requirements noted above, and a considerable number of issues remained, including the use of

Received: January 3, 2019

DOI: 10.1021/acs.oprd.9b00004
Org. Process Res. Dev. XXXX, XXX, XXX−XXX

Scheme 1. (a) Enzyme-Coupled and (b) Bifunctional Enzyme-Mediated Biocatalytic Process for 3-Quinuclidinone Bioconversion and Cofactor Regeneration

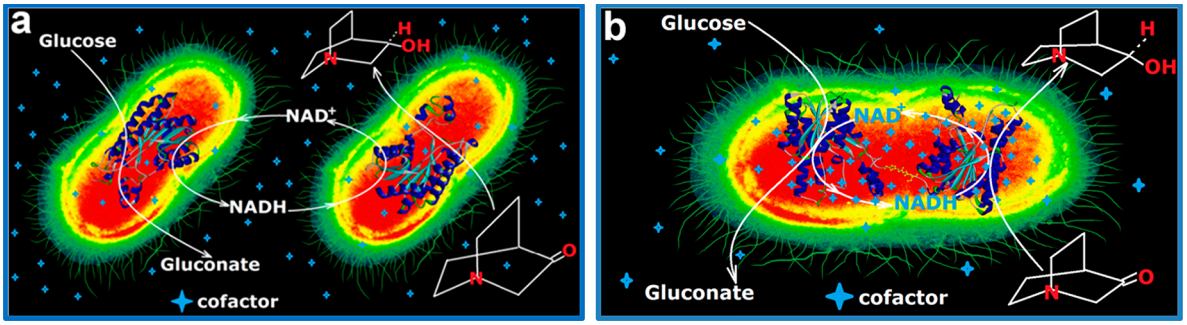

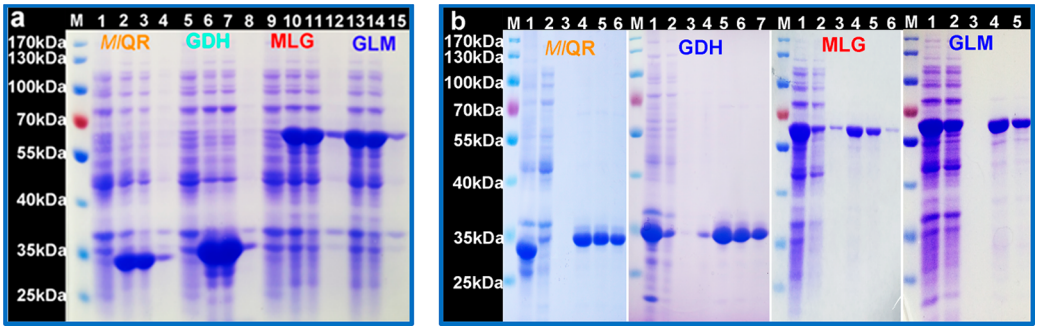

Figure 1. SDS-PAGE analysis of *Ml*QR, GDH, MLG, and GLM expression and purification. (a) Expression, Lane M, protein molecular weight markers; Lane 1−4, Lane 5−8, Lane 9−12, and Lane 13−15, the *E. coli* cells inducted before and after with 0.2 mM IPTG for 36 h, the lysate supernatant and precipitate for *E. coli*-*Ml*QR, *E. coli*-GDH, *E. coli*-MLG, and *E. coli*-GLM, respectively. (b) Purification, Lane 1−2, the lysate supernatant and flow-through fractions, Lane 3, washing-step fractions, Lane 4−6/7/5, elution-step fractions for *E. coli*-*Ml*QR, *E. coli*-GDH, *E. coli*-MLG, and *E. coli*-GLM, respectively.

two separate enzymes, more expensive cofactor $NADP^+$, and large amount of organic solvent, poor biocatalytic efficiency, therefore resulting in a prolonged conversion time. Overcoming these issues to obtain high product titer, productivity, and yield is still a formidable challenge.

As an alternative to using two separate enzymes and further improving catalytic efficiency, an artificial bifunctional enzyme can be constructed whereby two distant genetic elements are connected by a short linker sequence to yield a single polypeptide with two active sites.[29] The close proximity of the active centers in the bifunctional enzyme can reduce transfer distance of intermediates and increase the probability that a intermediate undergoes a sequential reaction step before diffusing into the bulk, therefore leading to the improvement of catalytic efficiency by 1−2 orders of magnitude over the free subunit.[30−33] For example, Iturrate et al.[33] constructed a bifunctional aldolase/kinase enzyme which exhibited an improved biocatalytic efficiency and a 20-fold increase in the reaction rate over the parent enzymes. Daniel et al.[34] has also demonstrated that genetically fusing Baeyer−Villiger monooxygenases with phosphite dehydrogenase make it a valuable tool for cofactor regeneration. More importantly, this method can reduce the number of enzymes which participate in the bioconversion reaction and avoid the purification of enzyme which is thought to be technically and economically challenging.[33,35] Due to these potential advantages, bifunctional enzymes have been utilized to synthesize chiral alcohol.[36−39] However, one disadvantage of formate dehydrogenase (FDH) used for the cofactor regeneration is that it is less active, less stable, and recycles only NAD^+.

Herein, we created a highly efficient bifunctional enzyme which exhibited good catalytic activities for (*R*)-3-quinuclidinol synthesis and cofactor regeneration of great capacity in the same polypeptide chain (Scheme 1b), and further simplified the biocatalytic behavior of the conventional enzyme-coupled process (Scheme 1a). This method may be useful for designing an all-purpose tailor-made self-sufficient two-in-one biocatalyst for the desired asymmetric reduction reactions requiring cofactor regeneration such as C═O and C═C bond reductions, reductive aminations, and so on at high substrate loading.

RESULTS AND DISCUSSION

Expression and Purification of Recombinant Enzymes. To start, we chose 3-Quinuclidinone Reductases (*Ml*QR) from *Microbacterium luteolum* and GDH from *Bacillus megaterium* to engineer bifunctional enzymes by a flexible linker sequence (GGGGS),[40] namely, MLG and GLM (each arranged from N- to C-terminus). The constructed plasmids pET28a-*Ml*QR, pET28a-GDH, pET28a-MLG, and pET28-GLM were respectively transformed to the host strains *E. coli* BL21(DE3). Each recombinant enzyme was successfully overexpressed in soluble form. The apparent molecular weight of MLG and GLM was estimated to be about 56 kDa, consisting of *Ml*QR (~26 kDa), GDH (~28 kDa), the linker (~0.4 kDa) and the His_6 tag (~0.9 kDa) as judged from SDS-PAGE analysis (Figure 1a). *E. coli* cells expressing corresponding enzyme were respectively denoted as *E. coli*-*Ml*QR, *E. coli*-GDH, *E. coli*-MLG, and *E. coli*-GLM, and directly employed for bioconversion process. Initial screening experiments suggested that both *E. coli*-MLG and *E. coli*-GLM exhibited

DOI: 10.1021/acs.oprd.9b00004
Org. Process Res. Dev. XXXX, XXX, XXX−XXX

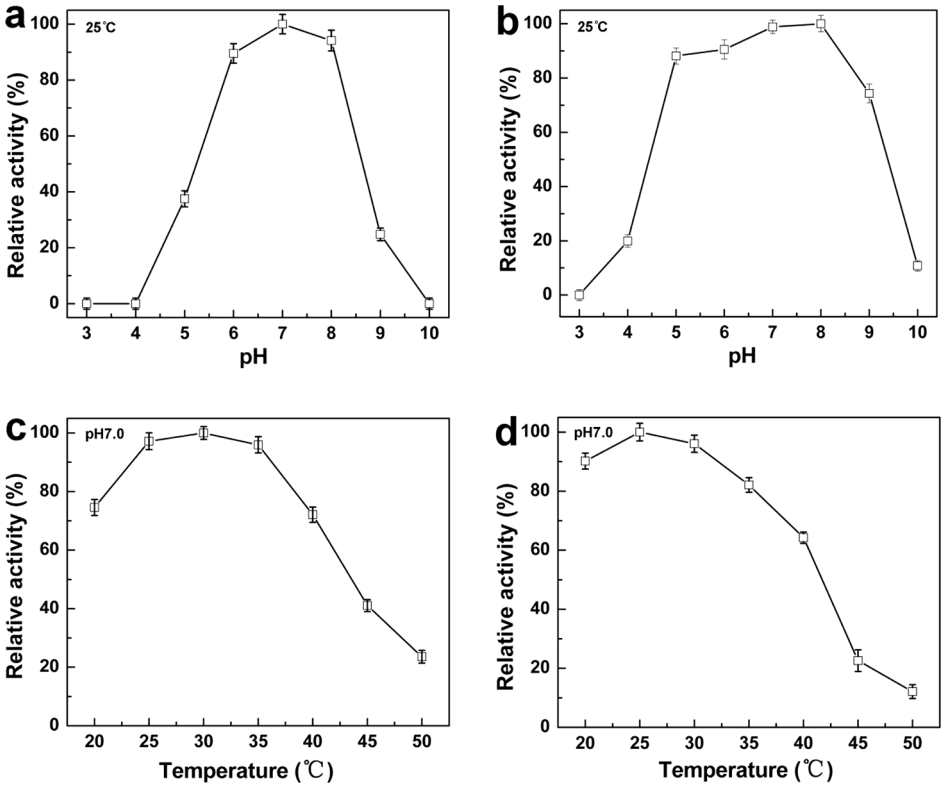

Figure 2. Effects of pH and temperature on the activity of ketoreductase (a, c) and cofactor regenerating enzyme (b, d) in the bifunctional enzyme MLG, respectively.

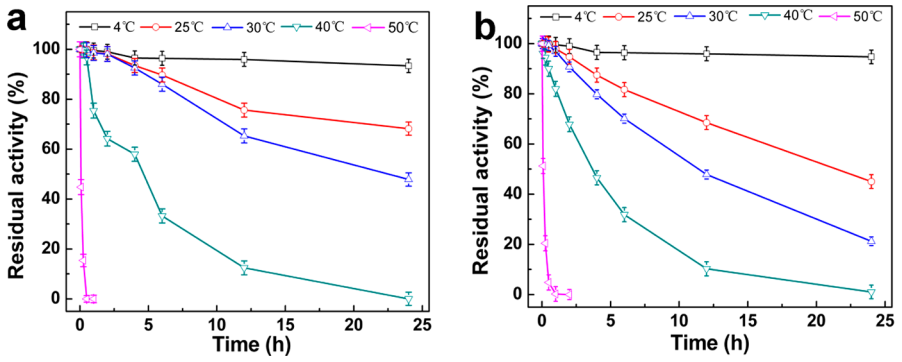

Figure 3. Thermostability of bifunctional enzyme MLG according to the determination of the activity of ketoreductase (a) and cofactor regenerating enzyme (b) in the MLG.

higher biocatalytic activity toward 3-quinuclidinone than a combination of the two native enzymes (*E. coli-Ml*QR and *E. coli*-GDH). And among the two bifunctional fusion enzymes, the *E. coli*-MLG displayed much better catalytic activity (see the Supporting Information, Table S1), and therefore was purified by single-step Ni^{2+} affinity chromatography (Figure 1b). The purified MLG was identified by Triple-TOF LC−MS, the peptide fragments were well matched with the target enzyme, further verifying that the bifunctional enzyme had the MLG expected features. The peptides identified can be collated, represented as a list of monoisotopic MW covering the major part of the amino acid sequence of MLG (see the Supporting Information, Figure S1−S2).

Activity Assays. To investigate the influence of pH and temperature on ketoreductase activity and cofactor regenerating enzyme activity in the bifunctional enzyme MLG, the enzyme MLG was incubated in PBS of 100 mM with different pH at 25 °C. After 0.5 h, the enzyme activity was measured. As can be seen from Figure 2a, ketoreductase (*Ml*QR) in the bifunctional enzyme MLG had the highest activity at pH 7.0, while cofactor regenerating enzyme (GDH) in the MLG presented a better pH tolerance ranging from 5.0 to 8.0 (Figure 2b). In the temperature stability experiments, the enzyme MLG was incubated in a preheated water bath at different temperatures (20−50 °C) and pH 7.0. As shown in Figure 2c and 2d, the ketoreductase in the bifunctional enzyme MLG exhibited a good temperature tolerance in the range of 25−35 °C. The activity of cofactor regenerating enzyme in the MLG was good at 25−30 °C, and the activity decreased significantly with increase in temperature.

Activity assays suggested that the enzyme MLG retained both activities with 3678 U/g for ketoreductase and 5070 U/g for cofactor regenerating enzyme, and the *Ml*QR and GDH

DOI: 10.1021/acs.oprd.9b00004
Org. Process Res. Dev. XXXX, XXX, XXX−XXX

Table 1. Summary of the Kinetic Constants of the Native Enzymes and Bifunctional Enzyme MLG

								MLG	
	RrQR	QNR	BacC	DnTR1	ArQR	*Ml*QR	GDH	*Ml*QR	GDH
K_m (mM)	145	6.5	13.8	8.71	0.4	3.54	0.65	12.06	1.62
K_{cat}/K_m (S^{-1} mM^{-1})	n.d[a]	5.6	0.08	0.0032	290	4.59	3.92	0.39	6.08
ref.	17	19	19	16	22	this study			

[a]n.d = not determined.

domains in the bifunctional enzyme exhibited similar thermostabilities to the native enzymes (Figure 3).

Steady-State Kinetic Assays. Steady-state kinetic analysis of the catalytic activities of ketoreductase and cofactor regenerating enzyme in the bifunctional enzyme MLG revealed that the fusion of GDH with *Ml*QR did not significantly affect either K_m or K_{cat} of GDH subunits in the MLG (Table 1, and see the Supporting Information Figure S3). However, both constants were modified for *Ml*QR subunits activity. The K_{cat} decrease of 3.5 times and the K_m increase resulted in a loss of K_{cat}/K_m of *Ml*QR subunits activity in the MLG of about 1 order of magnitude. The decrease in catalytic activities may be mainly due to the fact that some active sites of *Ml*QR subunits in the MLG were inaccessible for 3-quinuclidinone. However, the observed kinetic parameters allow its use in 3-quinuclidinone bioconversion.

Proximity Effect Study. To investigate the proximity effect, two sets of biotransformation reactions were concurrently performed according to the process shown in Scheme 1. Remarkably, the overall rate of 3-quinuclidinone bioconversion catalyzed by *E. coli*-MLG was about 3 fold higher than that by the combination of *E. coli*-*Ml*QR and *E. coli*-GDH (Figure 4), demonstrating that the catalytic activities of *Ml*QR

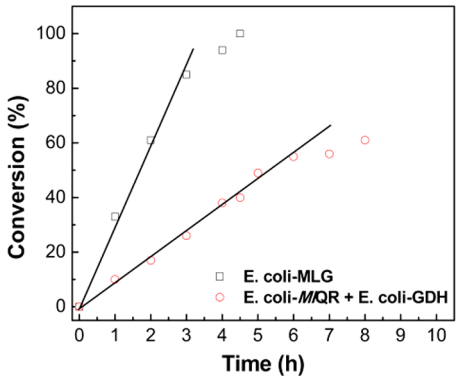

Figure 4. Asymmetric synthesis of (*R*)-3-quinuclidinol catalyzed by self-sufficient whole-cell *E. coli*-MLG or a combination of *E. coli*-*Ml*QR and *E. coli*-GDH. The slopes of the straight lines represent the overall rate of (*R*)-3-quinuclidinol formation.

and GDH in vivo were not impaired by the fusion, which was significantly important for preparative applications. The result could be attributed to the close proximity of the active sites in the fusion enzyme MLG. When the bioconversion was implemented by coupling two strains (Scheme 1a), the high mass transfer resistance resulted in the low catalytic efficiency, and the biocatalytic process was generally too complex for industrial application. However, when the process was performed in a single strain (Scheme 1b), a lower transit time which the cofactors produced by GDH subunits in MLG reached the *Ml*QR active sites in MLG, and higher local concentration of cofactors significantly reduced mass transfer problem and increased the probability of cofactors undergoing subsequent bioconversion before escaping by diffusion.[31,33]

Synthetic Application of the Self-Sufficient Whole-Cell Biocatalysts. A robust and efficient biocatalyst should show good biocatalytic performance. Therefore, the bioconversion reaction conditions including pH, temperature, the mole ratio of glucose to substrate, and cofactor concentration were first optimized. As shown in Figure 5, the optimum reaction conditions were 7.0, 30 °C, 1.5, and 0.2 mM, respectively. To further assess the catalytic performance of the self-sufficient whole-cell biocatalysts, all of the biotransformation reaction was performed in optimized reaction conditions in aqueous buffer solution. It was found that the conversion reaction proceeded highly efficiently at a substrate concentration of 81 g/L in the presence of very small amounts of cofactor providing the desired (*R*)-3-quinuclidinol with 100% conversion and an enantioselectivity of 100% ee (Table 2, entry 1) after 0.5 h, suggesting that the self-sufficient biocatalysts had good catalytic activity for 3-quinuclidinone. The substrate loading was then increased to 162 g/L under the same reaction conditions; the transformation was completed easily within 1.5 h (Table 2, entry 2). In a progressive manner, 243 g/L substrates which reached to the highest substrate loading ever reported[22] were added, still affording the desired product with a conversion of 100% and 100% ee at 2.5 h (Table 2, entry 3). When the biocatalysts reduced by half, the substrate was still completely reduced to afford 100% ee and >99% conversion within 5.5 h (Table 2, entry 4). Further reaction was performed at constant substrate without any external cofactor, and only 61% conversion was obtained even if the reaction time prolonged to 24 h (Table 2, entry 5). Our observation that the internal cofactor of the *E. coli* cells was insufficient for high substrate loading suggested that the amount of the cofactor should at least allow their use in catalytic instead of stoichiometric quantities. So a sufficient supply of cofactor in the same biocatalysts was a prerequisite for true preparative applications.

Then the reaction proceeded at 324 g/L of substrate, and still 100% substrate was converted to the product within 3.5 h with 100% ee (Table 2, entry 6). A bold attempt was made to proceed at impressive substrate loading (486 g/L) in the presence of 0.2 mM cofactor. Remarkably, the biotransformation of substrate still reached 100% in less than 5.5 h (Table 2, entry 7). The space-time yield (sty) of (*R*)-3-quinuclidinol and the total turnover number (TTN) respectively reached 1505.5 g L^{-1} d^{-1} and 15 000, which were the highest ever reported (Table 3). The time course of bioconversion demonstrated that faster bioconversion rate was achieved with increasing the amount of cofactor or biocatalysts used (Figure 6). To adapt biocatalysis, whether it uses whole cells or isolated enzymes, for industrial production, it should meets or exceeds these targets: ≥100 g/L substrate loading, ≥98% conversion, ≥99% ee, ≤5g/L biocatalyst loading, and ≤24 h of reaction time.[41]

DOI: 10.1021/acs.oprd.9b00004
Org. Process Res. Dev. XXXX, XXX, XXX−XXX

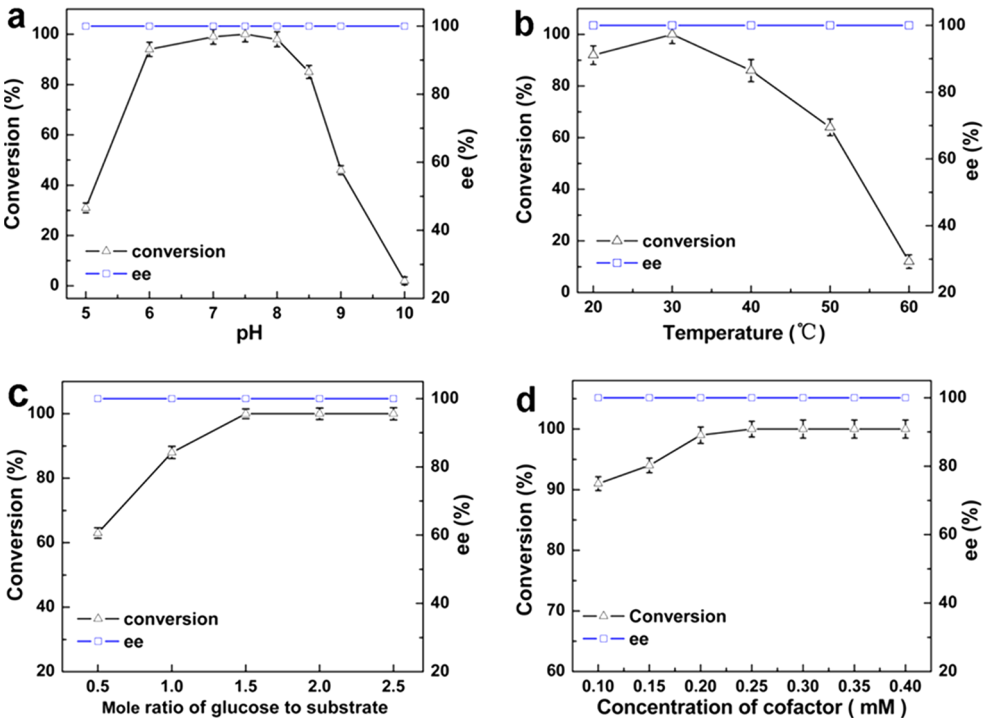

Figure 5. Influence of pH (a), temperature (b), the mole ratio of glucose to substrate (c), and cofactor concentration (d) on the catalytic performance of self-sufficient whole-cell biocatalysts.

Table 2. Asymmetric Reduction of 3-Quinuclidinone Using Whole-Cell Self-Sufficient Biocatalysts

entry	substrate (g/L)	cells (g/L)	NAD^+ (mM)	NADH (mM)	time (h)	conversion (%)	ee (%)
1	81	8.0	0.1	0.1	0.5	100	100
2	162	8.0	0.1	0.1	1.5	100	100
3	243	8.0	0.1	0.1	2.5	100	100
4	243	4.0	0.1	0.1	5.5	>99	100
5	243	8.0	0.0	0.0	24	61	100
6	324	8.0	0.1	0.1	3.5	100	100
7	486	8.0	0.1	0.1	5.5	100	100
8	486	8.0	0.05	0.05	8.5	100	100

Strikingly, even if the amount of the cofactor was reduced by half (Table 2, entry 8) compared with that of previous batch, still giving 100% conversion and 100% ee within 8.5 h. The sty of (*R*)-3-quinuclidinol still reached 974.2 g L^{-1} d^{-1}. Obviously, this biocatalytic process has well fulfilled these requirements.[41] In addition, the self-sufficient biocatalysts could be lyophilized and conveniently stored at −20 °C for months without significant activity loss, which was beneficial for long storage

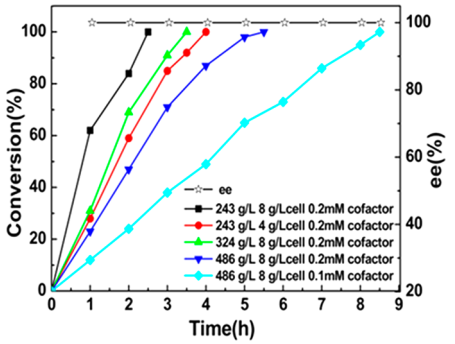

Figure 6. Time course of biotransformation of 3-quinuclidinone by self-sufficient whole-cell biocatalyst in the presence of cofactor and 1.5 equiv glucose at pH 7.0.

(see the Supporting Information, Figure S4). GC analysis was used to determine the ee value of the product (see the Supporting Information, Figure S5). ^{1}H NMR and ^{13}C NMR spectrum further confirmed the results (see the Supporting Information, Figure S6−S7).

Table 3. Comparison of Self-Sufficient Whole-Cell Biocatalyst *E. coli*-MLG with Other 3-Quinuclidinone Reductase

	substrate (g/L)	cells (g/L)	cofactor	time (h)	conversion (%)	ee (%)	sty (g L^{-1} d^{-1})	ref.
RrQR	100	15	NADPH	21	100	>99.9	90[a]	17
QNR	51	n.d.[b]	NADH	12	100	>99.9	80[a]	19
BacC	51	n.d.[b]	NADH	12	94	>99.9	75[a]	19
ADHs variant	113	n.d.[b]	NADH	22	89	>99	n.d.[b]	20
WY1202 cell	16	85	n.d.[b]	48	95.3	>99	6[a]	15
Mucor piriformis	2.0	n.d.[b]	n.d.[b]	288	73	96	n.d.[b]	16
ArQR	242	10	NADH	4.5	100	>99.9	916	22
MLG	486	8	NADH	5.5	100	100	1505.5	this study

[a]Data taken from ref 22. [b]Not determined.

DOI: 10.1021/acs.oprd.9b00004
Org. Process Res. Dev. XXXX, XXX, XXX−XXX

Large-Scale Synthesis of (*R*)-3-Quinuclidinol by the Self-Sufficient Whole-Cell Biocatalysts. The high substrate loading, enantioselectivities and conversion along with the short transformation period allowed a fast scale-up of the biocatalytic process. We conducted the bioconversion of 3-quinuclidinone on a 10 L scale at a substrate concentration of 3.0 M in the presence of the catalytic quantities of cofactor. A conversion of 100%, isolated yield of about 91% and >99.8% ee in good agreement with the previously reported results[22] were obtained after about 6 h at 8 g/L of dry biomass. The scalability of the self-sufficient biocatalyst demonstrated promising potential for large-scale synthesis of (*R*)-3-quinuclidinol.

CONCLUSIONS

In summary, we have devised a practical biocatalytic reduction system suitable for (*R*)-3-quinuclidinol synthesis in aqueous reaction medium and that proceeds at impressive substrate loading. The established method might be useful as an all-purpose biocatalyst for asymmetric reduction reactions requiring cofactor regeneration such as C═O and C═C bond reductions, reductive amination reactions, and so on. Now, we are further optimizing the catalytic efficiency of the newly developed self-sufficient whole-cell biocatalysts for final application in the large-scale synthesis of (*R*)-3-quinuclidinol, essential for production of solifenacin, palonosetron, revatropate, and aclidinium, with better clinical outcome than those currently available.

MATERIALS AND METHODS

Materials. All the recombinant plasmids were provided by Taihe (Beijing, China). Complete His-Tag Purification Resin was supplied by Roche Diagnostics GmbH (Mannheim, Germany). Competent *E. coli* BL21 (DE3) was purchased from Tiangen (Beijing, China). Pageruler prestained protein ladder was purchased from Thermo Fisher Scientific (Waltham, USA). Reagents used for sodium dodecyl sulfate polyacrylamide gel electrophoresis (SDS-PAGE) analysis and other commercial chemicals were the highest purity available and from Sigma (Shanghai, China) Ultrapure water used for the throughout experimental study was from Millipore system (Bedford, USA).

Expression and Purification of Recombinant Enzyme. 3-Quinuclidinone reductases (*Ml*QR) from *Microbacterium luteolum* and glucose dehydrogenase (GDH) from *Bacillus megaterium* were chosen to construct the bifunctional enzymes, namely, MLG (linked at C-terminal of *Ml*QR with N-terminal of GDH) and GLM (linked at N-terminal of *Ml*QR with C-terminal of GDH), by a flexible linker sequence (GGGGS).[40] The parent genes mlqr and gdh, fused genes mlg and glm, were linked to expression plasmid pET28a, respectively. The recombinant plasmid named as pET28a-*Ml*QR, pET28a-GDH, pET28a-MLG, and pET28-GLM were respectively transformed into competent *E. coli* BL21 (DE3) cells. A colony was cultured in 5 mL of Luria−Bertani (LB) broth (1% tryptone, 0.5% yeast extract, 1% NaCl) with 100 μg/mL of kanamycin with shaking at 37 °C overnight. The seed culture was then inoculated into 200 mL LB medium containing 100 μg/mL kanamycin and grown at 37 °C until OD_{600} reached 0.6. Then enzyme expression was induced with 0.2 mM IPTG (isopropyl β-D-thiogalactoside) at 20 °C for further 36 h. After that, the culture was centrifuged at 10 000 rpm during 10 min at 4 °C and washed with ice phosphate buffered saline (PBS) buffer. The resulting pellet was directly used or frozen at −20 °C or treated with lysozyme and DNase for purification and activity test.

Recombinant Enzyme Analysis. Recombinant enzyme-tagged with 6× His was purified by His-Tag Resin. Typically, 2 mL of native lysate were incubated for 2 h with 0.5 mL of Ni^{2+} resin pre-equilibrated with buffer A (150 mM NaCl, 50 mM Tris-HCl, pH8, 2 mM DTT) containing 10 mM imidazole with shaking. Unbound material was washed off with buffer A and the adsorbed-enzyme was eluted with the same buffer supplemented with an increasing gradient of imidazole from 100 to 500 mM. The bands on stained SDS-PAGE gels corresponding to the putative MLG were carefully excised, destained, and digested at 37 °C with trypsin overnight. Peptide mass fingerprint assays were performed by Triple-TOF 5600 LC−MS analysis system (ABSCIEX, USA) at Chongqing Medical University, Chongqing, China. Data were analyzed with the online tool Peptide Mass (http://web.expasy.org/peptide_mass/).

SDS-PAGE was performed using 12% and 5% acrylamide in the resolving and stacking gels, respectively, and gels were stained with Coomassie brilliant blue R-250.

Enzyme Activity Test. Bradford protein assay was performed to determine the enzyme concentration using bovine serum albumin as a standard.[42]

Enzyme activity was spectrophotometrically measured at room temperature by monitoring the absorbance at 340 nm (ε^{340}_{NADH} = 6220 M^{-1} cm^{-1}) corresponding to the change in NADH concentration by adding the substrate 3-quinuclidinone (10 μmol) or glucose (3 μmol), a coenzyme NADH (0.1 μmol) or NAD^+ (0.1 μmol), and an appropriate amount of enzymes (*Ml*QR, GDH, and the bifunctional enzymes) to 100 mM PBS (pH7.0) in a total volume of 1 mL according to the previously reported method.[19,43] The rate of absorbance decrease or increase is proportional to the enzyme activity (U) for reduction of 3-quinuclidinone to corresponding (*R*)-3-quinuclidinol or oxidation of glucose to gluconate.

Influences of pH and Temperature on the Enzyme Activity and Stability. The optimum pH and temperature were investigated at different pH ranging from 3.0 to 10.0 at 25 °C, different temperatures in the range of 20−50 °C at pH 7.0 using standard activity assays. The thermostability of bifunctional enzyme MLG was assayed by incubating in PBS (pH7.0) at varied temperatures (4, 25, 30, 40, and 50 °C) for 24 h. During this period, samples were withdrawn, and the residual activity was assayed under standard conditions.

Steady-State Kinetic Assays. Steady-state kinetic assays with MLG were determined in 6-well plates in a total volume of 1.0 mL at 25 °C. Measurements of kinetic parameters for MLG were carried out at different substrate concentrations. The catalytic constant (k_{cat}) is the result of dividing the V_{max} by the molar concentration of enzyme.

Proximity Effect Study. To investigate the influence of proximity effect on biotransformation reaction, the rate of biotransformation reaction mediated by a combination of whole-cells *E. coli*-*Ml*QR and *E. coli*-GDH or self-sufficient whole-cell biocatalysts *E. coli*-MLG was determined and compared under the same conditions. In both cases, 1.8 U of ketoreductase activity (*Ml*QR) and 2.5 U of cofactor regenerating enzyme activity (GDH) were used. A slightly higher amount of MLG in terms of mg of protein was used to fit the U of activity. Thus, 0.55 mg of MLG was utilized by a

DOI: 10.1021/acs.oprd.9b00004
Org. Process Res. Dev. XXXX, XXX, XXX−XXX

total of 4.7 U for the sum of ketoreductase activity in MLG (2.0 U) and cofactor regenerating enzyme activity in MLG (2.7 U). The reactions were carried out at 30 °C in 10 mL of PBS (100 mM, pH 7.0) containing 0.5 mmol of 3-quinuclidinone·HCl, 0.75 mmol of D-glucose, 0.1 mM NAD^+, and 0.1 mM NADH, and an appropriate amount of lyophilized cells. At different time, 100 μL aliquots were withdrawn to quantify the formed (*R*)-3-quinuclidinol by GC analysis.

Synthetic Application of the Self-Sufficient Whole-Cell Biocatalysts. To fully display catalytic performance of self-sufficient whole-cell biocatalysts, the bioconversion reaction conditions including pH ranging from 5.0 to 9.0, temperature ranging from 20 to 60 °C, the mole ratio of glucose to substrate in the range of 0.5−2.5, cofactor concentration ranging from 0.1 to 0.4 mM, and the substrate concentration (81−486 g/L) were first optimized. The influence of long-period storage on biocatalysts activity was also studied. Typical biotransformation reaction catalyzed by the whole-cell self-sufficient biocatalysts was carried out in 10.0 mL of PBS (100 mM, pH 7.0) containing 0.81 g 3-quinuclidinone, 1.2 g glucose, 0.1 mM NAD^+, 0.1 mM NADH, and 0.08 g of lyophilized cells as biocatalysts with continuous shaking at 125 rpm. After the biotransformation completed, the pH value of the resulting reaction mixture was adjusted 12.0. The product was extracted twice with *n*-butanol, and the organic layer was thoroughly dried with anhydrous Na_2SO_4. Then the solution was analyzed by GC as described below.

Biotransformation at 10 L Scale. The biotransformations were carried out at 30 °C, and pH at 7−8 was maintained by adding 5 M NaOH with a mechanical stirrer. 3-Quinuclidinone·HCl (3 M, 4860 g), glucose (4.5 M, 8100 g), cofactor (0.2 mM, 1.33 g), and lyophilized cells (8.0 g/L) were mixed in a total of 10 L PBS (100 mM, pH 7.0).

Product Isolation. Product isolation was carried out as described previously[22,44] with slight modifications. Briefly, after 6 h, 400 g trifluoroacetic acid was added to the reaction mixture and then heated until boiling. The boiled mixture was cooled to room temperature followed by filtrating with the aid of active carbon to remove proteins. The filtrate was pH adjusted to 12.0 with NaOH, concentrated, and extracted three times with an equal volume of *n*-butanol. The combined organic phases of three *n*-butanol extractions were concentrated. After azeotropic dehydration by the cycle of addition of about 28 L toluene, the formed (*R*)-3-quinuclidinol product was completely dissolved at 90 °C in toluene, followed by heating filtration to remove the residual inorganic salts. About 3430 g of white (*R*)-3-quinuclidinol crystals were obtained by cooling, collecting, and drying the filtrate under vacuum reaction.

Analytical Procedures. ^1H and ^{13}C NMR spectra were recorded on Bruker Ascend III HD (600 MHz) using $CHCl_3$ as solvent. Enantiomeric excess (ee) was determined according to the previously reported method,[43,45] on a Clarus 580 GC system (PerkinElmer, USA) equipped with a chiral capillary column (HYDRODEX-β-6-TBDM, 25 m × 0.25 mm × 0.25 μm, Macherey−Nagel) and flame-ionization detector with injector and detector at 220 and 250 °C, respectively, and column temperature at 180 °C. The space-time yield (sty) was calculated according to the following equation.

$$\text{sty} = \frac{m \times M_{\text{3-quinuclidinol}} \times C \times Y}{M_{\text{3-quinuclidinone·HCl}} \times V \times D} \quad (1)$$

m: substrate weight, *M*: molecular weight, *C*: conversion yield, *Y*: total yield of biotransformation reaction, *V*: total volume of biotransformation reaction, *D*: time of biotransformation reaction.

The total turnover number (TTN) were calculated by

$$\text{TTN} = \frac{m_{\text{3-quinuclidinol}}\ (\text{mol})}{m_{\text{cofactor}}\ (\text{mol})} \quad (2)$$

■ ASSOCIATED CONTENT

Supporting Information

The Supporting Information is available free of charge on the ACS Publications website at DOI: 10.1021/acs.oprd.9b00004.

Experimental information, peptide mass fingerprint, MS spectra, substrate kinetic of activities, long-term storage stability, and analysis of the ee values and copies of ^1H and ^{13}C NMR of the product (PDF)

■ AUTHOR INFORMATION

Corresponding Author

*E-mail: li_wei@cqmu.edu.cn. Phone: +86 23 6848 5161.

ORCID

Wei Li: 0000-0003-2283-0091

Notes

The authors declare no competing financial interest.

■ ACKNOWLEDGMENTS

This work was supported by Chongqing Municipality Education Commission (KJ1400212), the Municipal Science and Technology Committee of Chongqing (CSTC2014jcyjA0019), and School of Pharmacy, Chongqing Medical University.

■ REFERENCES

(1) Ni, Y.; Xu, J. H. Biocatalytic ketone reduction: A green and efficient access to enantiopure alcohols. *Biotechnol. Adv.* **2012**, *30*, 1279−1288.

(2) Huisman, G. W.; Liang, J.; Krebber, A. Practical chiral alcohol manufacture using ketoreductases. *Curr. Opin. Chem. Biol.* **2010**, *14*, 122−129.

(3) Hanson, R. L.; Goldberg, S. L.; Guo, Z.; Tully, T. P.; Goswami, A.; Ye, X. Y.; Robl, J. A.; Patel, R. N. Enzymatic reduction of adamantanones to chiral adamantanol intermediates for the synthesis of 11-β-hydroxysteroid dehydrogenase inhibitors. *Org. Process Res. Dev.* **2014**, *18*, 960−968.

(4) Tang, Y.; Zhang, G.; Wang, Z.; Liu, D.; Zhang, L.; Zhou, Y.; Huang, J.; Yu, F.; Yang, Z.; Ding, D. Efficient synthesis of a (*S*)-fluoxetine intermediate using carbonyl reductase coupled with glucose dehydrogenase. *Bioresour. Technol.* **2018**, *250*, 457−463.

(5) Thompson, M.; Penafiel, I.; Cosgrove, S. C.; Turner, N. J. Biocatalysis using immobilised enzymes in continuous flow for the synthesis of fine chemicals. *Org. Process Res. Dev.* **2019**, *23*, 9−18.

(6) Naito, R.; Yonetoku, Y.; Okamoto, Y.; Toyoshima, A.; Ikeda, K.; Takeuchi, M. Synthesis and Antimuscarinic Properties of Quinuclidin-3-yl 1, 2, 3, 4- Tetrahydroisoquinoline-2-carboxylate Derivatives as Novel Muscarinic Receptor Antagonists. *J. Med. Chem.* **2005**, *48*, 6597−6606.

(7) Prat, M.; Fernández, D.; Buil, M. A.; Crespo, M. I.; Casals, G.; Ferrer, M.; Tort, L.; Castro, J.; Monleón, J. M.; Gavaldà, A.; Miralpeix, M.; Ramos, I.; Doménech, T.; Vilella, D.; Antón, F.; Huerta, J. M.;

DOI: 10.1021/acs.oprd.9b00004
Org. Process Res. Dev. XXXX, XXX, XXX−XXX

Espinosa, S.; López, M.; Sentellas, S.; González, M.; Albertí, J.; Segarra, V.; Cárdenas, A.; Beleta, J.; Ryder, H. Discovery of novel quaternary ammonium derivatives of (3R)-quinuclidinol esters as potent and long-acting muscarinic antagonists with potential for minimal systemic exposure after inhaled administration: identification of (3R)-3-{[hydroxy(di-2-thienyl)acetyl]oxy-1-(3-phenoxypropyl)-1-azoniabicyclo[2.2.2] octanebromide (aclidinium bromide). *J. Med. Chem.* **2009**, *52*, 5076−5092.

(8) Montuschi, P.; Ciabattoni, G. Bronchodilating Drugs for Chronic Obstructive Pulmonary Disease: Current Status and Future Trends. *J. Med. Chem.* **2015**, *58*, 4131−4164.

(9) Gralla, R.; Lichinitser, M.; Van der Vegt, S.; Sleeboom, H.; Mezger, J.; Pe-schel, C.; Tonini, G.; Labianca, R.; Macciocchi, A.; Aapro, M. Palonosetron improves prevention of chemotherapy-induce nausea and vomiting following moderately emetogenic chemotherapy: results of a double-blind randomized phase III trial comparing single doses of palonosetron with ondansetron. *Ann. Oncol.* **2003**, *14*, 1570−1577.

(10) Rabe, K. F; Watz, H. Chronic obstructive pulmonary disease. *Lancet* **2017**, *389*, 1931−1940.

(11) Marsh, K.; Zaiser, E.; Orfanos, P.; Salverda, S.; Wilcox, T.; Sun, S.; Dixit, S. Evaluation of COPD treatments: A multicriteria decision analysis of aclidinium and tiotropium in the United States. *Value Health* **2017**, *20*, 132−140.

(12) Tsutsumi, K.; Katayama, T.; Utsumi, N.; Murata, K.; Arai, N.; Kurono, N.; Ohkuma, T. Practical asymmetric hydrogenation of 3-Quinuclidinone catalyzed by the XylSkewphos /PICA-Ruthenium (II) complex. *Org. Process Res. Dev.* **2009**, *13*, 625−628.

(13) Arai, N.; Akashi, M.; Sugizaki, S.; Ooka, H.; Inoue, T.; Ohkuma, T. Asymmetric Hydrogenation of Bicyclic Ketones Catalyzed by BINAP/IPHAN-Ru (II) Complex. *Org. Lett.* **2010**, *12*, 3380−3383.

(14) Nomoto, F.; Hirayama, Y.; Ikunaka, M.; Inoue, T.; Otsuka, K. Practical chemoenzymatic process to access (*R*)-quinuclidin-3-ol on scale. *Tetrahedron: Asymmetry* **2003**, *14*, 1871−1877.

(15) Wang, Y.; Li, J.; Wu, Q.; Zhu, D. Microbial stereospecific reduction of 3-quinuclidinone with newly isolated nocardia sp. and rhodococcus erythropolis. *J. Mol. Catal. B: Enzym.* **2013**, *88*, 14−19.

(16) Kolet, S. P.; Jadhav, D. D.; Priyadarshini, B.; Swarge, B. N.; Thulasiram, H. V. Fungi mediated production and practical purification of (*R*)-(−)-3-quinuclidinol. *Tetrahedron Lett.* **2014**, *55*, 5911−5914.

(17) Uzura, A.; Nomoto, F.; Sakoda, A.; Nishimoto, Y.; Kataoka, M.; Shimizu, S. Stereoselective synthesis of (*R*)-3-quinuclidinol through asymmetric reduction of 3-quinuclidinone with 3-quinuclidinone reductase of rhodotorula rubra. *Appl. Microbiol. Biotechnol.* **2009**, *83*, 617−626.

(18) Isotani, K.; Kurokawa, J.; Itoh, N. Production of (*R*)-3-Quinuclidinol by E. coli biocatalysts possessing NADH-dependent 3-Quinuclidinone reductase (QNR or bacC) from *Microbacterium luteolum* and leifsonia alcohol dehydrogenase (LSADH). *Int. J. Mol. Sci.* **2012**, *13*, 13542−13553.

(19) Isotani, K.; Kurokawa, J.; Suzuki, F.; Nomoto, S.; Negishi, T.; Matsuda, M.; Itoh, N. Gene Cloning and Characterization of Two NADH-Dependent 3-Quinuclidinone Reductases from *Microbacterium luteolum* JCM9174. *Appl. Environ. Microbiol.* **2013**, *79*, 1378−1384.

(20) Spickermann, D.; Hausmann, S.; Degering, C.; Schwaneberg, U.; Leggewie, C. Engineering of highly selective variants of parvibaculum lavamentivorans alcohol dehydrogenase. *ChemBioChem* **2014**, *15*, 2050−2052.

(21) Chen, W.; Cheng, X.; Zhou, Z.; Liu, J.; Wang, H. Molecular cloning and characterization of a tropinone reductase from Dendrobium nobile Lindl. *Mol. Biol. Rep.* **2013**, *40*, 1145−1154.

(22) Zhang, W. X.; Xu, G. C.; Huang, L.; Pan, J.; Yu, H. L.; Xu, J. H. Highly Efficient Synthesis of (*R*)-3-Quinuclidinol in a Space-Time Yield of 916 g L^{-1} d^{-1} Using a New Bacterial Reductase ArQR. *Org. Lett.* **2013**, *15*, 4917−4919.

(23) Jia, Z.; Ma, H.; Huang, Y.; Huang, Y.; Ren, P.; Song, S.; Hu, M.; Tao, Y. Production of (*R*)-3-quinuclidinol by a whole-cell biocatalyst with high efficiency. *Biocatal. Biotransform.* **2018**, *36*, 316−323.

(24) Noyori, R.; Ohkuma, T. Asymmetric Catalysis by Architectural and Functional Molecular Engineering: Practical Chemo- and Stereoselective Hydrogenation of Ketones. *Angew. Chem., Int. Ed.* **2001**, *40*, 40−73.

(25) Gröger, H.; Chamouleau, F.; Orologas, N.; Rollmann, C.; Drauz, K.; Hummel, W.; Weckbecker, A.; May, O. Enantioselective Reduction of Ketones with "Designer Cells" at High Substrate Concentrations: Highly Efficient Access to Functionalized Optically Active Alcohols. *Angew. Chem., Int. Ed.* **2006**, *45*, 5677−5681.

(26) Kataoka, M.; Kita, K.; Wada, M.; Yasohara, Y.; Hasegawa, J.; Shimizu, S. Novel bioreduction system for the production of chiral alcohols. *Appl. Microbiol. Biotechnol.* **2003**, *62*, 437−445.

(27) Kizaki, N.; Yasohara, Y.; Hasegawa, J.; Wada, M.; Kataoka, M.; Shimizu, S. Synthesis of optically pure ethyl (*S*)-4-chloro-3-hydroxybutanoate by Escherichia coli transformant cells coexpressing the carbonyl reductase and glucose dehydrogenase genes. *Appl. Microbiol. Biotechnol.* **2001**, *55*, 590−595.

(28) Xu, Q.; Tao, W. Y.; Huang, H.; Li, S. Highly efficient synthesis of ethyl (*S*)-4-chloro-3-hydroxybutanoate by a novel carbonyl reductase from Yarrowia lipolytica and using mannitol or sorbitol as cosubstrate. *Biochem. Eng. J.* **2016**, *106*, 61−67.

(29) Bülow, L.; Ljungcrantz, P.; Mosbach, K. Preparation of a soluble biofunctional enzyme by gene fusion. *Nat. Biotechnol.* **1985**, *3*, 821−823.

(30) Hyde, C. C.; Ahmed, S. A.; Padlan, E. A.; Miles, E. W.; Davies, D. R. Three-dimensional structure of the tryptophan synthase alpha 2 beta2 multienzyme complex from Salmonella typhimurium. *J. Biol. Chem.* **1988**, *263*, 17857−17871.

(31) Conrado, R. J.; Varner, J. D.; DeLisa, M. P. Engineering the spatial organization of metabolic enzymes: mimicking nature's synergy. *Curr. Opin. Biotechnol.* **2008**, *19*, 492−499.

(32) Castellana, M.; Wilson, M. Z.; Xu, Y.; Joshi, P.; Cristea, I. M.; Rabinowitz, J. D.; Gitai, Z.; Wingreen, N. S. Enzyme clustering accelerates processing of intermediates through metabolic channeling. *Nat. Biotechnol.* **2014**, *32*, 1011−1018.

(33) Iturrate, L.; Sánchez-Moreno, I.; Doyagüez, E. G.; García-Junceda, E. Substrate channeling in an engineered bifunctional aldolase/kinase enzyme confers catalytic advantage for C−C bond formation. *Chem. Commun.* **2009**, *13*, 1721−1723.

(34) Torres Pazmino, D. E.; Snajdrova, R.; Baas, B.-J.; Ghobrial, M.; Mihovilovic, M. D.; Fraaije, M. W. Self-sufficient Baeyer-Villiger monooxygenases: effective coenzyme regeneration for biooxygenation by fusion engineering. *Angew. Chem., Int. Ed.* **2008**, *47*, 2275−2278.

(35) Vahidi, A. K.; Yang, Y.; Ngo, T. P. N.; Li, Z. Simple and Efficient Immobilization of Extracellular His-Tagged Enzyme Directly From Cell Culture Supernatant as Active and Recyclable Nano-biocatalyst: High-Performance Production of Biodiesel from Waste Grease. *ACS Catal.* **2015**, *5*, 3157−3161.

(36) Holsch, K.; Weuster-Botz, D. Enantioselective reduction of prochiral ketones by engineered bifunctional fusion proteins. *Biotechnol. Appl. Biochem.* **2010**, *56*, 131−140.

(37) Li, B.; Li, Y.; Bai, D.; Zhang, X.; Yang, H.; Wang, J.; Liu, G.; Yue, J.; Ling, Y.; Zhou, D.; Chen, H. Whole-cell biotransformation systems for reduction of prochiral carbonyl compounds to chiral alcohol in Escherichia coli. *Sci. Rep.* **2015**, *4*, 6750.

(38) Suhrer, I.; Haslbeck, M.; Castiglione, K. Asymmetric synthesis of a fluoxetine precursor with an artificial fusion protein of a ketoreductase and a formate dehydrogenase. *Process Biochem.* **2014**, *49*, 1527−1532.

(39) Calam, E.; González-Roca, E.; Fernández, R.; Dequin, S.; Parés, X.; Virgili, A.; Biosca, J. A. Enantioselective Synthesis of Vicinal (R, R)-Diols by Saccharomyces cerevisiae Butanediol Dehydrogenase. *Appl. Environ. Microbiol.* **2016**, *82*, 1706−1721.

(40) Chen, X.; Zaro, J. L.; Shen, W. C. Fusion protein linkers: Property, design and functionality. *Adv. Drug Delivery Rev.* **2013**, *65*, 1357−1369.

DOI: 10.1021/acs.oprd.9b00004
Org. Process Res. Dev. XXXX, XXX, XXX−XXX

(41) Luetz, S.; Giver, L.; Lalonde, J. Engineered Enzymes for Chemical Production. *Biotechnol. Bioeng.* **2008**, *101*, 647−653.
(42) Bradford, M. M. A Rapid Method for the Quantitation of Microgram Quantities of Protein Utilizing the Principle of Protein-Dye Binding. *Anal. Biochem.* **1976**, *72*, 248−254.
(43) Yu, M.; Liu, D.; Sun, L.; Li, J.; Chen, Q.; Pan, L.; Shang, J.; Zhang, S.; Li, W. Facile fabrication of 3D porous hybrid sphere by co-immobilization of multi-enzyme directly from cell lysates as an efficient and recyclable biocatalyst for asymmetric reduction with coenzyme regeneration in situ. *Int. J. Biol. Macromol.* **2017**, *103*, 424−434.
(44) Yamamoto, H.; Ueda, M.; Pan, R.; Hamatani, T. Methods for producing optically active alcohols. Patent US2005/0227336A1, 2005.
(45) Preeti, R.; Pandey, A.; Binod, P. Microbial production of ketoreductases: Development of a novel high-throughput screening method. *Bioresour. Technol.* **2017**, *242*, 319−323.

DOI: 10.1021/acs.oprd.9b00004
Org. Process Res. Dev. XXXX, XXX, XXX−XXX